Defect Engineered Single-Layer MoS_2 Dendrites as an Efficient Electrocatalyst for Hydrogen Evolution Reaction

Wenshuo Xu*, Sha Li**, Mauro Pasta*** and Jamie H. Warner****

*Oxford Suzhou Centre for Advanced Research, Jiangsu, China; University of Oxford, Oxford, United Kingdom, wenshuo.xu@oxford-oscar.cn
**University of Oxford, Oxford, United Kingdom, sha.li@materials.ox.ac.uk
***University of Oxford, Oxford, United Kingdom, mauro.pasta@materials.ox.ac.uk
****Oxford Suzhou Centre for Advanced Research, Jiangsu, China; University of Oxford, Oxford, United Kingdom, jamie.warner@materials.ox.ac.uk

ABSTRACT

Dendritic structures display a high density of edge sites, which are electrocatalytically active in hydrogen evolution reaction (HER). However, given that the basal plane of 2H-phase MoS_2 synthesized by chemical vapor deposition (CVD) is inert, activation strategies have been explored to utilize 2H-phase MoS_2 as an efficient electrocatalyst toward applications in HER. Here single-layer MoS_2 dendrites grown by CVD were engineered with oxygen plasma so that numerous defects are generated prevailingly across its basal plane. We observe PL enhancement in the defect regions, caused by the heavy p-type doping and the conversion from trion to exciton and the suppression of nonradiative recombination of excitons. More importantly, the as-treated MoS_2 exhibits improved HER performance along with high cycling stability, owning to the great addition of sulfur vacancies and the increase in edge site density.

Keywords: molybdenum disulfide (MoS_2), monolayer dendrites, defect engineering, hydrogen evolution reaction (HER), electrocatalyst

1 INTRODUCTION

Nowadays, developing technologies are demanded for clean energy with renewable resources. Water splitting is the most convenient and promising method to produce hydrogen (H_2). Platinum (Pt), which has a small negative hydrogen absorption energy and minimum overpotential, is the best-known catalyst for hydrogen evolution reaction (HER). However, the high cost of Pt greatly limits its applications. Thus, intensive efforts have been contributed to the investigation of non-noble-metal alternatives, and MoS_2 has been demonstrated to be a suitable candidate. The electrochemically active sites of MoS_2 toward HER basically include its edge sites and sulfur vacancies, whereas the basal plane of 2H-phase MoS_2 produced by chemical vapor deposition is inert [1–4]. Efforts have been made extensively to enrich the edge sites and activate the basal plane of MoS_2 [5–8]. Amongst these novel methods, the construction of dendritic structures during CVD synthesis has gained much attention [5,6]. It is believed that the growth of dendrites is mainly initiated from the twin defects in MoS_2 nuclei, and the growth mode is strongly dependent on the in-situ vapor ratio of S/Mo [5,9]. Also, single-layer MoS_2 have more advantages. The reason is that the electron hoping barrier is minimized and some other fascinating properties such as photoluminescence (PL) can be maximized when it is thinned down to a monolayer. In this work, to obtain affordable electrocatalyst with high efficiency for HER, we applied defect engineering to the MoS_2 single-layer dendrites, so that their HER performance is improved because of the increase in the active site density. In addition, we show that the induced p-type doping and oxygen bonding lead to an enhancement in the PL intensity.

2 EXPERIMENTAL METHODS

The single-layer MoS_2 dendrites were grown by atmospheric pressure chemical vapor deposition (APCVD) method with the precursors of molybdenum trioxide (MoO_3) and sulfur (S) and carrier gases of argon (Ar). Silicon chips with a 300 nm oxide layer (SiO_2/Si) were used as the substrate. The growth procedure and parameters can be found in our earlier publication [6]. The defect engineering for the as-synthesized MoS_2 was conducted with oxygen plasma, which lasted for 5 min and the excitation power to ionize the oxygen is constantly 60 mW. The MoS_2 samples were imaged at room temperature using an optical microscope and SEM (Hitachi-4300, 3.0 kV accelerating voltage), and ADF-STEM (JEOL ARM-200F STEM with a CEOS aberration corrector, 80 kV accelerating voltage) instruments. A dwell time of 32 μS and a pixel size of 0.0073−0.015 nm px^{-1} were applied for the ADF-STEM imaging, along with a 30 μm CL aperture, 24.6 mrad convergence semiangle, 12 pA beam current, and 39−156 mrad inner acquisition angle. The ADF-STEM images were subjected to a Gaussian smooth. PL spectroscopy was performed with a JY Horiba LabRAM ARAMIS imaging confocal Raman microscope. A 12.5 mW, 532 nm (2.33 eV) diode laser was employed for excitation, which was focused down to a ~1 μm spot. The acquisition times for spectra and maps were 1 and 0.1 s, respectively. An AFM

instrument was used to measure the layer thickness by Asylum Research MFP-3D in the AC mode with a silicon AC-160TS cantilever (Olympus, spring constant of ~42 N m^{-1}, and resonant frequency of ~300 kHz). The catalytic performance of the CVD-grown MoS_2 was measured in a three-electrode system, using the monolayer MoS_2 transferred onto a glassy carbon plate as the working electrode, a carbon rod as the counter electrode, and Ag/AgCl/KCl (3 M) as the reference electrode. A defined working area of the sample was immerged into a 0.5 M H_2SO_4 N_2-purged solution for HER activities. The potentials were calibrated to a reversible hydrogen electrode (E (RHE) = E (Ag/AgCl/KCl (3 M)) + 0.21 − 0.059·pH). The linear sweep voltammetry (LSV) was conducted under quasi-equilibrium conditions at 1 mV s^{-1} and the cyclic voltammetry (CV) was applied at a scan rate of 100 mV s^{-1}. Electrochemical impedance spectroscopy (EIS) was measured by sweeping the frequency from 200000 Hz to 1 Hz with a perturbation voltage amplitude of 10 mV.

3 RESULTS AND DISCUSSION

Below we present the characterization and HER testing results for the as-synthesized MoS_2 and discuss about its growth mechanism, electrocatalytic behavior, etc.

3.1 APCVD Growth of Single-Layer MoS_2 Dendrites

Figure 1a depicts the APCVD used in the present work for growing monolayer MoS_2. Large-area MoS_2 nanosheets are produced by a three-stage growth (Figure 1b). Slightly Excessive precursor feedstocks are provided by a high gas flow rate during the initial stage to form nuclei. After that, the main growth starts under a lower gas flow rate and proceeds by consuming the excess precursors at local sites. Then, the gas flow rate is further decreased so that the atoms residing on the domain surfaces can migrate freely to the adjacent edges. The temperature is simultaneously decreased to reduce both the feedstock of MoO_3 and the sublimation of as-produced MoS_2. The relative concentrations of the gaseous precursors vary greatly on different substrate surfaces. The atom ratio of Mo/S can determine the shape of the resulting MoS_2 domains. The low Mo/S ratio on the substrate surface typically gives rise to MoS_2 dendrites with a high branching degree (Figure 1c,d). Figure 1d presents an abundance of edge sites accommodated by the dendritic pattern. As the growth system is rich in sulfur, the nucleation density of MoS_2 relies on the concentration of MoO_3, which is very low near the tube wall. Lateral growth is favored at the nuclei with lower densities, giving a larger domain size of the dendritic MoS_2 on the bottom substrate. The optimized CVD procedure and substrate construction allow the production of large-area, highly dendritic MoS_2 monolayers with the arm length up to ~390 μm.

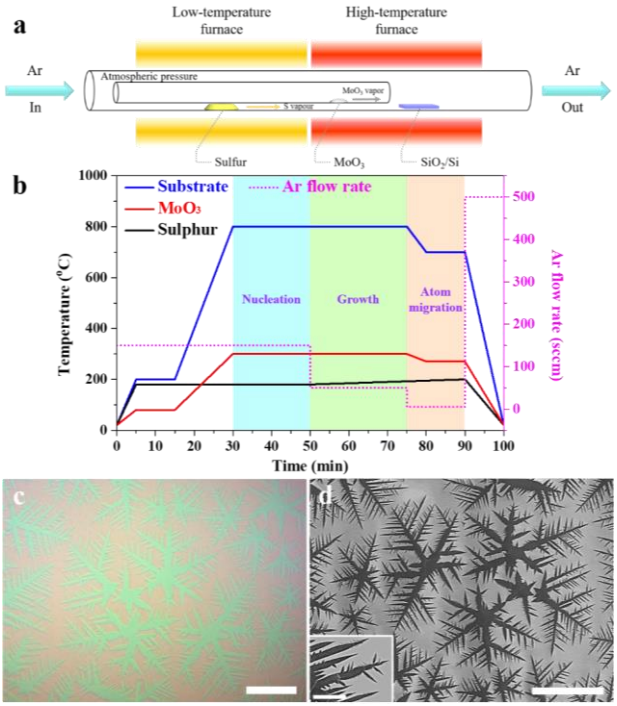

Figure 1: (a) CVD setup and (b) Profiles of the programmed temperature and carrier gas flow rate for the synthesis of single-layer MoS_2 dendrites. (c) Optical microscopy images and (d) scanning electron microscopy (SEM) images for the as-grown dendritic single-layer MoS_2. Scale bar: 200 μm. The inset of panel (f) shows the fine detail of a dendrite tip; scale bar: 10 μm.

3.2 Defect Engineering of the MoS_2 Dendrites

To improve the HER performance of the CVD-grown single-layer MoS_2 dendrites, we treated the sample with 60 mW-ionized oxygen plasma for 5 min. The pulsing supply of oxygen species can efficiently eliminate the MoS_2 nanosheet, especially the S atoms. As shown in Figure 2, two types of electrocatalytically active sites are generated, i.e., microcracks (Figure 2a) and sulfur vacancies (i.e., loss of sulfur atoms in the MoS_2 crystal lattice, Figure 2b). Also, some of the produced single-layer dendritic MoS_2 domains exhibit six-fold symmetric backbones due to the cyclic twin defects [9]. These dendrites show similar observations, i.e., the presence of microcracks and microholes, as can be seen in the inset of Figure 2a.

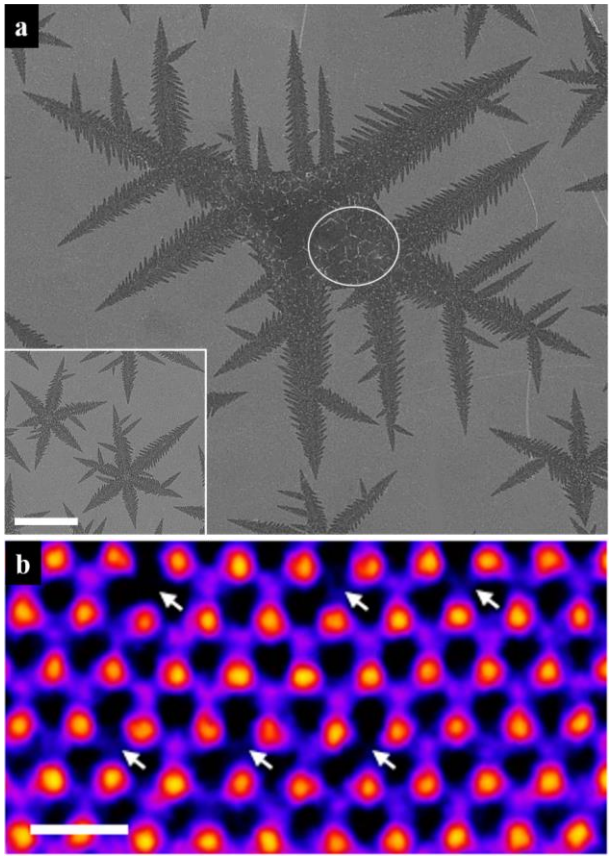

Figure 2. (a) SEM image and (b) STEM image of the defect engineered single-layer MoS_2 dendrites. The white circle in panel a and the white arrows in panel b indicate the as-generated microcracks and sulfur vacancies, respectively. Scale bar: (a) 10 μm and 60 μm for the inset; (b) 1 nm.

To further demonstrate the generated defects, we conducted PL spectroscopy on the single-layer MoS_2 dendrites. Figure 3a manifests a strong PL enhancement in the MoS_2 treated with oxygen plasma, which can be ascribed to defect engineering and oxygen bonding. The PL mapping clearly reveals that the PL intensity is greatly increased at the regions of microcracks and sulfur vacancies formed by the oxygen plasma. After taking the laser spot size into consideration, the enhancement is estimated to be about 5 times. This could result from the heavy p-type doping induced by the oxygen chemical adsorption and the conversion from trion to exciton, and the suppression of nonradiative recombination of excitons at the defect sites [10]. Since the intensity ratio of A to A^- is an indicator of the doping level of MoS_2, Lorentzian fitting has been performed to both the pristine MoS_2 (Figure 3b) and the defected engineered MoS_2 (Figure 3c), and the evident increased A/A^- ratio accompanied by a blue shift of the PL peak position verifies the resultant p-doping in the MoS_2. Furthermore, the uniformity of the total integrated PL intensity across the dendritic domain is also different. In this aspect, the dendritic MoS_2 domains with six-fold symmetric backbones were comparatively investigated (Figure 3d–g). For the pristine MoS_2 in Figure 3d, a uniform PL map is attained (Figure 3e), whereas for the defect engineered counterpart in Figure 3f, PL enhancement is observed primarily in the central body and secondly along the edges. The enhanced PL demonstrates again the involvement of defects, which are accommodated mainly by the basal plane of MoS_2, and moreover, it shows how the PL mapping can be utilized to identify the preferential oxidation sites in the single-layer MoS_2.

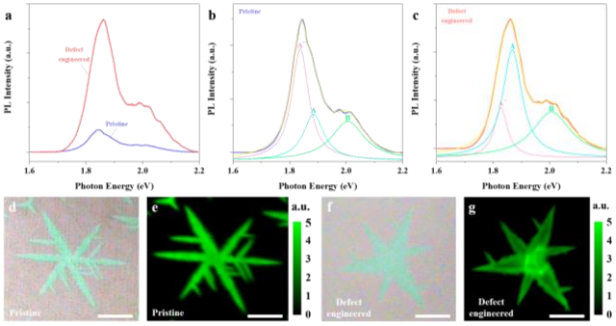

Figure 3: (a) Averaged PL spectra of the pristine and the defect engineered single-layer MoS_2 dendrites, for which the Lorentzian fitting is shown in (b) and (c), respectively. (d,f) Optical microscopic image of a pristine (d) and a defect engineered (f) single-layer MoS_2 dendrites, shown with (e,g) the corresponding 2D maps of the total integrated PL intensity. Scale bar: 30 μm.

3.3 Electrochemical Measurements

We tested the HER activities of the defect engineered single-layer MoS_2 dendrites, for which the results are presented in Figure 4. Both the increased current density at certain overpotential in the cathodic polarization curves (Figure 4a) and the decreased slopes in the Tafel plots (Figure 4b) verified the improved efficiency for hydrogen production, which means that the generation of active sites contributed to an enhanced electrocatalysis for the HER. The semiarc at the low frequency region is an indicator of the kinetic control in the electrode process, and any mass transfer control is excluded, which would otherwise give an additional straight line with a 45° angle at the low frequency region. It can be inferred from the smaller semiarc radius in Figure 4c for the dendritic morphology and additional microcracks/defects that the increased density of electron hopping sites can permit a reduced charge transfer resistance (R_{ct}) across the MoS_2–electrolyte interface. This can promote the rate-determining step in the HER, i.e., proton discharge (Volmer reaction: $H_3O^+ + e^- \rightarrow H_{ads} + H_2O$) in our case, and thereby improve the catalytic activity of MoS_2. Additionally, the HER activities can keep stable up to 3,000 times cycling (Figure 4d). These results also prove that the oxygen plasma treatment have, to some extent, activated the basal plane of the CVD-grown 2H-phase MoS_2.

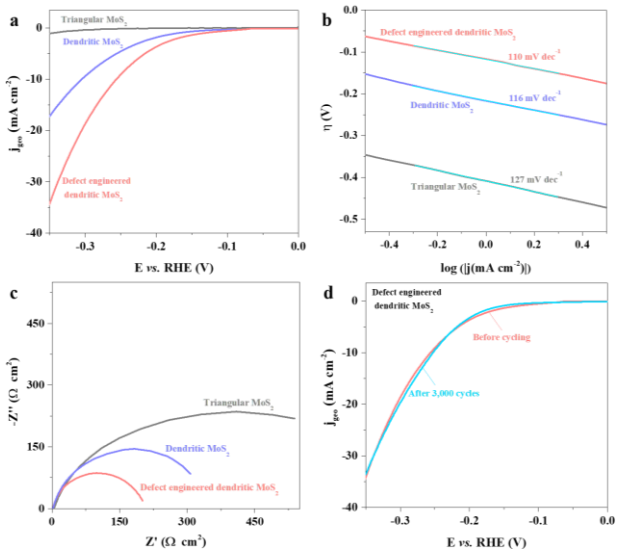

Figure 4: HER activities of the single-layer MoS_2 grown by APCVD. (a) Cathodic polarization curves. (b) Tafel plots with the slopes obtained via linear fits. (c) Nyquist plots at 10 mV showing the impedance of the electrochemical system. (d) Cathodic polarization curves for which cycling procedures were applied.

4 CONCLUSION

Highly dendritic single-layer MoS_2 with a large domain size has been synthesized through APCVD technique. Further, a facile and feasible method has been developed to manipulate the microstructure of such 2H-phase MoS_2. This has been achieved by engineering the CVD-grown dendritic MoS_2 with oxygen plasma, in which way numerous microcracks and sulfur vacancies were produced so that the electrocatalytically inert basal plane of the 2H-phase MoS_2 was activated for HER. The PL mapping verifies that the oxidation occurred preferentially at the central body and along the edges of the MoS_2 dendrites, which led to an enhancement in the overall PL intensity at these sites. More importantly, the HER performance of the MoS_2 dendrites have been improved as a result of the increased density of active sites. Our work provides a sensible route to facilitate the commercial viability of water electrolysis application.

5 ACKNOWLEDGEMENTS

W.X. and J.H.W. thank the Suzhou Industrial Park, the Royal Society, and the European Research Council (Grant No. 725258 CoG 2016 LATO) for support.

REFERENCES

[1] T. F. Jaramillo, K. P. Jørgensen, J. Bonde, J. H. Nielsen, S. Horch and I. Chorkendorff, "Identification of Active Edge Sites for Electrochemical H_2 Evolution from MoS_2 Nanocatalysts," Science, 317, 100−102, 2007.

[2] H. Li, C. Tsai, A. L. Koh, L. Cai, A. W. Contryman, A. H. Fragapane, J. Zhao, H. S. Han, H. C. Manoharan, F. Abild Pedersen, J. K. Nørskov and Zheng, X, "Activating and Optimizing MoS_2 Basal Planes for Hydrogen Evolution through the Formation of Strained Sulphur Vacancies," Nat. Mater., 15, 48−53, 2016.

[3] Y. Yin, J. Han, Y. Zhang, X. Zhang, P. Xu, Q. Yuan, L. Samad, X. Wang, Y. Wang, Z. Zhang, P. Zhang, X. Cao, B. Song and S. Jin, "Contributions of Phase, Sulfur Vacancies, and Edges to the Hydrogen Evolution Reaction Catalytic Activity of Porous Molybdenum Disulfide Nanosheets," J. Am. Chem. Soc., 138, 7965−7972, 2016.

[4] G. Li, D. Zhang, Q. Qiao, Y. Yu, D. Peterson, A. Zafar, R. Kumar, S. Curtarolo, F. Hunte, S. Shannon, Y. Zhu, W. Yang and L. Cao, "All the Catalytic Active Sites of MoS_2 for Hydrogen Evolution," J. Am. Chem. Soc., 138, 16632−16638, 2016.

[5] Y. Zhang, Q. Ji, G.-F. Han, J. Ju, J. Shi, D. Ma, J. Sun, Y. Zhang, M. Li, X.-Y. Lang, Y. Zhang and Z. Liu, "Dendritic, Transferable, Strictly Monolayer MoS_2 Flakes Synthesized on $SrTiO_3$ Single Crystals for Efficient Electrocatalytic Applications," ACS Nano, 8, 8617–8624, 2014.

[6] W. Xu, S. Li, S. Zhou, J. K. Lee, S. Wang, S. G. Sarwat, X. Wang, H. Bhaskaran, M. Pasta, and J. H. Warner, "Large Dendritic Monolayer MoS_2 Grown by Atmospheric Pressure Chemical Vapor Deposition for Electrocatalysis," ACS Appl. Mater. Interfaces, 10, 4630–4639, 2018.

[7] S. Li, S. Wang, M. M. Salamone, A. W. Robertson, S. Nayak, H. Kim, S. E. Tsang, M. Pasta and J. H. Warner, "Edge Enriched 2D MoS_2 Thin Films Grown by Chemical Vapor Deposition for Enhanced Catalytic Performance," ACS Catal., 7, 877−886. 2017.

[8] G. Ye, Y. Gong, J. Lin, B. Li, Y. He, S. T. Pantelides, W. Zhou, R. Vajtai and P. M. Ajayan, "Defects Engineered Monolayer MoS_2 for Improved Hydrogen Evolution Reaction," Nano Lett., 16, 1097–1103, 2016.

[9] J. Wang, X. Cai, R. Shi, Z. Wu, W. Wang, G. Long, Y. Tang, N. Cai, W. Ouyang, P. Geng, B. N. Chandrashekar, A. Amini, N. Wang and C. Cheng, "Twin Defect Derived Growth of Atomically Thin MoS_2 Dendrites," ACS Nano, 12, 635−643, 2018.

[10] H. Nan, Z. Wang, W. Wang, Z. Liang, Y. Lu, Q. Chen, D. He, P. Tan, F. Miao, X. Wang, J. Wang and Z. Ni, "Strong Photoluminescence Enhancement of MoS_2 through Defect Engineering and Oxygen Bonding," ACS Nano, 8, 5738–5745, 2014.